

Turbo Receiver Design for MIMO Relay ARQ Transmissions

Halim Yanikomeroglu

Carleton University, Canada

A joint work with

Zakaria El-Moutaouakkil (Telecom Bretagne, France)

Tarik Ait-Idir (ExceliaCom Solutions, Morocco)

Samir Saoudi (Telecom Bretagne, France)

Global Communications Conference (GLOBCOM) 2012

5th December 2012

Outline

- 1 Cooperative Communications
- 2 Relay ARQ System
- 3 Information-Theoretic Analysis
- 4 Simulation Results I
- 5 Signal-Level Sub-Packet Combining
- 6 Simulation Results II
- 7 Conclusion and Perspectives
- 8 Related Works

Progress of wireless communications

- **1G** : (1980s ~ 1990s) wireless communications were based on **analogue systems**.
- **2G** : (1990s ~ 2000) such systems as GSM and IS-95 were defined, these systems were essentially designed for **voice and low data rate applications**.
- **3G** : (2000 ~ 2010) it addresses customer demands for **high-speed data communications** while the business focus has shifted from voice services to **multimedia communication applications over Internet**.
- **4G** : (Next few months) moving from standardization to deployment phase with the promise of providing **faster and more affordable wireless Internet connectivity**.

5G (beyond-4G) !?

5G Requirements Impacting on Physical Layer

- **Very high bit rates** (e.g. 100 Mb/s to 1 Gb/s) with **high user densities**.
- Ubiquitous coverage.
- Adaptive and self configuring to user needs and transmission environment.
- **Moderate cost**: terminal cost, power and battery requirements commensurate with required performance and data rate.

5G Requirements Impacting on Physical Layer

- **Very high bit rates** (e.g. 100 Mb/s to 1 Gb/s) with **high user densities**.
- **Ubiquitous coverage**.
- Adaptive and self configuring to user needs and transmission environment.
- **Moderate cost**: terminal cost, power and battery requirements commensurate with required performance and data rate.

5G Requirements Impacting on Physical Layer

- **Very high bit rates** (e.g. 100 Mb/s to 1 Gb/s) with **high user densities**.
- **Ubiquitous coverage**.
- **Adaptive and self configuring** to **user needs** and **transmission environment**.
- **Moderate cost**: terminal cost, power and battery requirements commensurate with required performance and data rate.

5G Requirements Impacting on Physical Layer

- **Very high bit rates** (e.g. 100 Mb/s to 1 Gb/s) with **high user densities**.
- **Ubiquitous coverage**.
- **Adaptive and self configuring** to **user needs** and **transmission environment**.
- **Moderate cost**: terminal cost, power and battery requirements commensurate with required performance and data rate.

5G Requirements Impacting on Physical Layer

- **Very high bit rates** (e.g. 100 Mb/s to 1 Gb/s) with **high user densities**.
- **Ubiquitous coverage**.
- **Adaptive and self configuring** to **user needs** and **transmission environment**.
- **Moderate cost**: terminal cost, power and battery requirements commensurate with required performance and data rate.

Goal \Rightarrow enabling the **4A** paradigm
“**any** rate, **any**time, **any**where, **affordable**”

5G Requirements Impacting on Physical Layer

- **Very high bit rates** (e.g. 100 Mb/s to 1 Gb/s) with **high user densities**.
- **Ubiquitous coverage**.
- **Adaptive and self configuring** to **user needs** and **transmission environment**.
- **Moderate cost**: terminal cost, power and battery requirements commensurate with required performance and data rate.

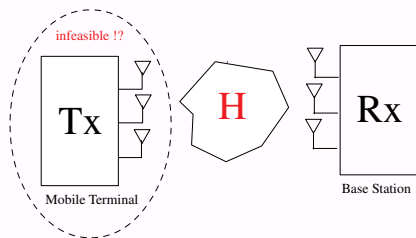
⇒ **Cooperative Relaying Concept**

5G Requirements Impacting on Physical Layer

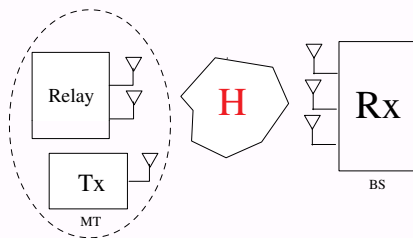
- **Very high bit rates** (e.g. 100 Mb/s to 1 Gb/s) with **high user densities**.
- **Ubiquitous coverage**.
- **Adaptive and self configuring** to **user needs** and **transmission environment**.
- **Moderate cost**: terminal cost, power and battery requirements commensurate with required performance and data rate.

⇒ **Cooperative Relaying Concept**

Constraint posed by 3G & 4G mobile terminals



3×3 MIMO System



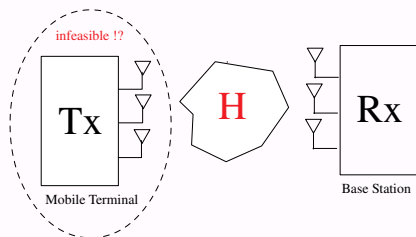
3×3 Virtual MIMO System

- In cellular Networks, it is not feasible to deploy several antennas at our mobile terminals !!

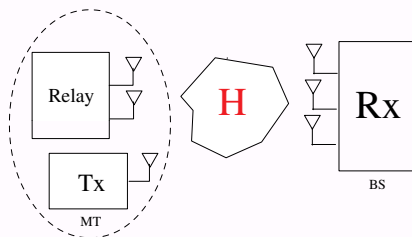
Solution

- Virtual MIMO has been proposed.
- ⇒ Cooperative Communication

Constraint posed by 3G & 4G mobile terminals



3×3 MIMO System



3×3 Virtual MIMO System

- In cellular Networks, it is not feasible to deploy several antennas at our mobile terminals !!

Solution

- Virtual MIMO has been proposed.
- ⇒ Cooperative Communication

Relay ARQ System Model

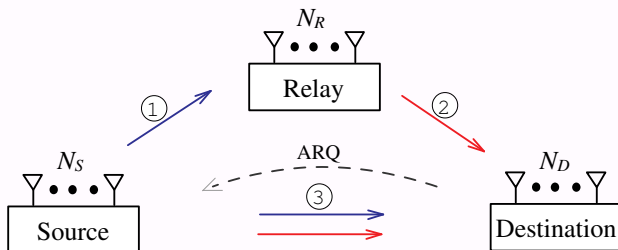


Fig. 1: Relay ARQ System Model.

Brief Description of the Concept

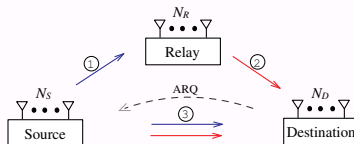


Fig. 1: Relay ARQ System Model

- Channel 1, channel 2, and channel 3 are regarded at k th transmission as a frequency selective fading MIMO channels having L_{SR} , L_{RD} , and L_{SD} independent paths, respectively.
- Each path is characterized by its quasi-static flat fading MIMO channel matrix $\mathbf{H}_l^{AB(k)} \in \mathbb{C}^{N_A \times N_B}$, for $l \in \{0, \dots, L_{AB} - 1\}$ where $A \in \{S, R\}$ and $B \in \{R, D\}$.
- Relaying works under the framework of half-duplex amplify-and-forward protocol.
- Packet re-transmissions follows the Chase-type ARQ mechanism.

Brief Description of the Concept

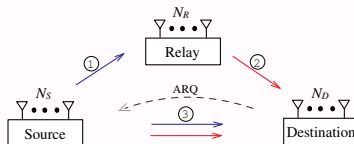


Fig. 1: Relay ARQ System Model

- Channel 1, channel 2, and channel 3 are regarded at k th transmission as a frequency selective fading MIMO channels having L_{SR} , L_{RD} , and L_{SD} independent paths, respectively.
- Each path is characterized by its quasi-static flat fading MIMO channel matrix $\mathbf{H}_l^{AB(k)} \in \mathbb{C}^{N_A \times N_B}$, for $l \in \{0, \dots, L_{AB} - 1\}$ where $A \in \{S, R\}$ and $B \in \{R, D\}$.
- Relaying works under the framework of half-duplex amplify-and-forward protocol.
- Packet re-transmissions follows the Chase-type ARQ mechanism.

Brief Description of the Concept

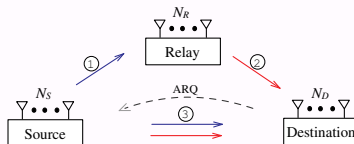


Fig. 1: Relay ARQ System Model

- Channel 1, channel 2, and channel 3 are regarded at k th transmission as a frequency selective fading MIMO channels having L_{SR} , L_{RD} , and L_{SD} independent paths, respectively.
- Each path is characterized by its quasi-static flat fading MIMO channel matrix $\mathbf{H}_l^{AB^{(k)}} \in \mathbb{C}^{N_A \times N_B}$, for $l \in \{0, \dots, L_{AB} - 1\}$ where $A \in \{S, R\}$ and $B \in \{R, D\}$.
- Relaying works under the framework of half-duplex amplify-and-forward protocol.
- Packet re-transmissions follows the Chase-type ARQ mechanism.

Brief Description of the Concept

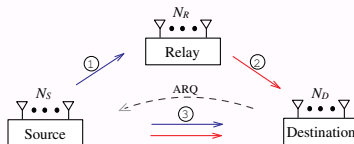


Fig. 1: Relay ARQ System Model

- Channel 1, channel 2, and channel 3 are regarded at k th transmission as a frequency selective fading MIMO channels having L_{SR} , L_{RD} , and L_{SD} independent paths, respectively.
- Each path is characterized by its quasi-static flat fading MIMO channel matrix $\mathbf{H}_l^{AB^{(k)}} \in \mathbb{C}^{N_A \times N_B}$, for $l \in \{0, \dots, L_{AB} - 1\}$ where $A \in \{S, R\}$ and $B \in \{R, D\}$.
- Relaying works under the framework of half-duplex amplify-and-forward protocol.
- Packet re-transmissions follows the Chase-type ARQ mechanism.

Brief Description of the Concept

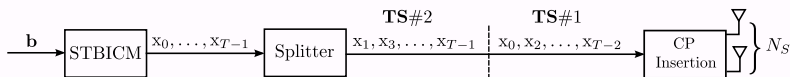


Fig. 2: Source node transmitter scheme.

Splitting Rule

- Upon the 1st transmission, node S generates according to an STBICM encoder the symbol packet

$$\mathbf{x} \triangleq [x_0, \dots, x_{T-1}] \in \mathbb{C}^{N_S \times T}. \quad (1)$$

- It is then splitted into two equally sized $N_S \times \frac{T}{2}$ sub-packets \mathbf{z}_1 and \mathbf{z}_2 constructed as

$$\begin{cases} z_{1,t} = x_{2t} & , \quad 0 \leq t \leq \frac{T}{2} - 1 \\ z_{2,t} = x_{2t+1} & , \quad 0 \leq t \leq \frac{T}{2} - 1 \end{cases}. \quad (2)$$

Brief Description of the Concept

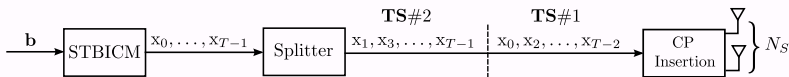


Fig. 2: Source node transmitter scheme.

Splitting Rule

- Upon the 1st transmission, node S generates according to an STBICM encoder the symbol packet

$$\mathbf{x} \triangleq [x_0, \dots, x_{T-1}] \in \mathbb{C}^{N_S \times T}. \quad (1)$$

- It is then splitted into two equally sized $N_S \times \frac{T}{2}$ sub-packets \mathbf{z}_1 and \mathbf{z}_2 constructed as

$$\begin{cases} z_{1,t} = x_{2t} & , \quad 0 \leq t \leq \frac{T}{2} - 1 \\ z_{2,t} = x_{2t+1} & , \quad 0 \leq t \leq \frac{T}{2} - 1 \end{cases}. \quad (2)$$

Relay ARQ Protocol

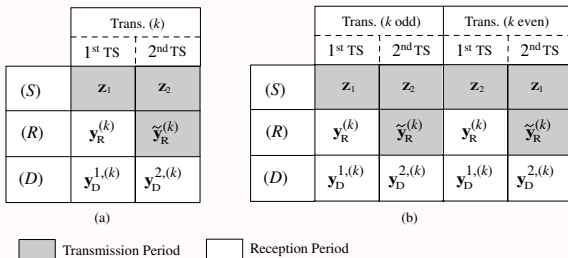


Fig. 3: Relay ARQ Protocol (a), Relay ARQ with Slot-Mapping Reversal (b) for $k = 1, \dots, K$.

Sub-Packets Slot Mapping is Fixed Fig. 3(a)

- \mathbf{z}_1 followed by \mathbf{z}_2 during the first and the second TS, respectively, for all the ARQ rounds.

Relay ARQ with Slot Mapping Reversal

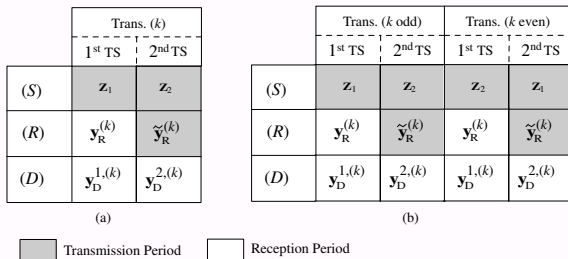


Fig. 3: Relay ARQ Protocol (a), Relay ARQ with Slot-Mapping Reversal (b) for $k = 1, \dots, K$.

Sub-Packets Slot Mapping is Reversed Fig. 3(b)

- Depending on the **transmission index parity**, sub-packets \mathbf{z}_1 and \mathbf{z}_2 are mapped onto either the first or the second time slot.

Sub-Packets ARQ Transmission Model (I)

During the 1st TS of ARQ round k :

$$\mathbf{y}_{R,t}^{(k)} = \sqrt{E_{SR}} \sum_{l=0}^{L_{SR}-1} \mathbf{H}_l^{SR(k)} \mathbf{z}_{1,(t-l) \bmod \frac{T}{2}} + \mathbf{n}_{R,t}^{(k)} \quad (3)$$

$$\mathbf{y}_{D,t}^{1,(k)} = \sqrt{E_{SD}} \sum_{l=0}^{L_{SD}-1} \mathbf{H}_{1,l}^{SD(k)} \mathbf{z}_{1,(t-l) \bmod \frac{T}{2}} + \mathbf{n}_{D,t}^{1,(k)} \quad (4)$$

- E_{SR} and E_{SD} are the energies capturing the effects of path loss and shadowing in channel 1 and 3, respectively.
- $\mathbf{n}_{B,t}^{(k)} \sim \mathcal{N}(\mathbf{0}_{N_B \times 1}, N_0 \mathbf{I}_{N_B})$ for $B \in \{R, D\}$.
- A cyclic prefix (CP) portion of length $L_{cp} = \max\{L_{SD}, L_{SR}, L_{RD}\}$ is appended to \mathbf{z}_1 and \mathbf{z}_2 upon their transmission.

AF function at the Relay node:

$$\begin{cases} \tilde{\mathbf{y}}_{R,t}^{(k)} = \gamma \mathbf{y}_{R,t}^{(k)} & t = 0, \dots, \frac{T}{2} - 1 \\ \gamma = 1/\sqrt{N_S E_{SR} + N_0} \end{cases} \quad (5)$$

Sub-Packets ARQ Transmission Model (II)

During the 2^{nd} TS of ARQ round k :

$$\mathbf{y}_{D,t}^{2,(k)} = \sum_{l=0}^{L_{max}-1} \tilde{\mathbf{H}}_l^{(k)} \mathbf{z}_{(t-l) \bmod \frac{T}{2}} + \tilde{\mathbf{n}}_{D,t}^{2,(k)} \quad (6)$$

where

$$\begin{cases} \mathbf{z}_t & \triangleq \begin{bmatrix} \mathbf{z}_{1,t} \\ \mathbf{z}_{2,t} \end{bmatrix} \in \mathcal{X}^{2N_S}, \\ L_{max} & \triangleq \max(L_{SD}, L_{SRD}), \text{ and } L_{SRD} = L_{SR} + L_{RD} - 1, \end{cases} \quad (7)$$

$$\tilde{\mathbf{H}}_l^{(k)} = \left[\gamma \sqrt{E_{SR} E_{RD}} \underline{\mathbf{H}}_l^{SRD(k)} \quad \sqrt{E_{SD}} \underline{\mathbf{H}}_{2,l}^{SD(k)} \right],$$

$$\tilde{\mathbf{n}}_{D,t}^{2,(k)} = \gamma \sqrt{E_{RD}} \sum_{l=0}^{L_{RD}-1} \mathbf{H}_l^{RD(k)} \mathbf{n}_{R,(t-l) \bmod \frac{T}{2}}^{(k)} + \mathbf{n}_{D,t}^{2,(k)}. \quad (8)$$

Sub-Packets ARQ Transmission Model (III)

At the end of the second slot node D builds up (jointly) the augmented size signal vector

$$\mathbf{y}_{D,t}^{equ(k)} \left\{ \begin{bmatrix} \mathbf{y}_{D,t}^{1,(k)} \\ \tilde{\mathbf{y}}_{D,t}^{2,(k)} \end{bmatrix} \right. = \sum_{l=0}^{Lmax-1} \mathbf{H}_l^{equ(k)} \mathbf{z}_{(t-l) \bmod \frac{T}{2}} + \mathbf{n}_{D,t}^{equ(k)}, \quad (9)$$

in which the k -parity $2N_D \times 2N_S$ equivalent MIMO channel matrix $\mathbf{H}_l^{equ(k)}$ has been carefully introduced with the following form

$$\begin{cases} \mathbf{H}_l^{equ(k)} = \begin{bmatrix} \mathbf{A} & \mathbf{0}_{N_D \times N_S} \\ \mathbf{B} & \mathbf{C} \end{bmatrix}, & k \text{ odd} \\ \mathbf{H}_l^{equ(k)} = \begin{bmatrix} \mathbf{0}_{N_D \times N_S} & \mathbf{A} \\ \mathbf{C} & \mathbf{B} \end{bmatrix}, & k \text{ even} \end{cases} \quad (10)$$

where,

$$\mathbf{A} = \sqrt{E_{SD}} \underline{\mathbf{H}}_{1,l}^{SD(k)}, \quad (11)$$

$$\mathbf{B} = \gamma \sqrt{E_{SR} E_{RD}} L^{-1} \underline{\mathbf{H}}_l^{SRD(k)}, \quad (12)$$

$$\mathbf{C} = \sqrt{E_{SD}} L^{-1} \underline{\mathbf{H}}_{2,l}^{SD(k)}. \quad (13)$$

Sub-Packets ARQ Transmission Model (III)

In a joint manner signal vector $\mathbf{y}_{D,t}^{equ(k)}$ is grouped with all the previously received signals $\mathbf{y}_{D,t}^{equ(k-1)}, \dots, \mathbf{y}_{D,t}^{equ(1)}$ to decode the data packet.

K ARQ rounds Transmission Model

This leads to the $2N_D k \times 2N_s$ block transmission model given by

$$\underbrace{\begin{bmatrix} \mathbf{y}_{D,t}^{equ(1)} \\ \vdots \\ \mathbf{y}_{D,t}^{equ(k)} \end{bmatrix}}_{\mathbf{y}_{D,t}^{equ,k}} = \sum_{l=0}^{L_{max}-1} \underbrace{\begin{bmatrix} \mathbf{H}_l^{equ(1)} \\ \vdots \\ \mathbf{H}_l^{equ(k)} \end{bmatrix}}_{\mathbf{H}_l^{equ,k}} \mathbf{z}_{(t-l) \bmod \frac{T}{2}} + \underbrace{\begin{bmatrix} \mathbf{n}_{D,t}^{equ(1)} \\ \vdots \\ \mathbf{n}_{D,t}^{equ(k)} \end{bmatrix}}_{\mathbf{n}_{D,t}^{equ,k}}. \quad (14)$$

Outage Probability

Definition (Pertaining to $K=1$)

The outage probability at a given signal-to-noise ratio (SNR) ρ , denoted by P_{out} , refers to the probability half of the information rate \mathcal{I} (the factor $\frac{1}{2}$ comes from the fact that one channel use of the equivalent received signal model (9) corresponds to two temporal channel uses), between transmitted block $\underline{\mathbf{z}}$ and received block $\underline{\mathbf{y}}_D^{equ,1}$, is below a target rate \mathcal{R} ,

$$P_{out}(\rho, \mathcal{R}) = \Pr \left\{ \frac{1}{2} \mathcal{I} \left(\underline{\mathbf{z}}; \underline{\mathbf{y}}_D^{equ,1} \mid \left\{ \mathbf{H}_l^{equ,1} \right\}, \rho \right) < \mathcal{R} \right\} \quad (15)$$

where

$$\underline{\mathbf{z}} = \begin{bmatrix} \mathbf{z}_1 \\ \vdots \\ \mathbf{z}_{\frac{T}{2}} \end{bmatrix}, \text{ and } \underline{\mathbf{y}}_D^{equ,1} = \begin{bmatrix} \mathbf{y}_{D,1}^{equ,1} \\ \vdots \\ \mathbf{y}_{D, \frac{T}{2}-1}^{equ,1} \end{bmatrix}.$$

Outage Probability

Generalization

To extend the previous formula on our ARQ relay system, we use the renewal theory as well as the observation that allows us to view the presented Chase-type ARQ mechanism, with a maximum number of rounds K , as a repetition coding scheme over K parallel sub-virtual channels. Accordingly, given the equivalent MIMO-ARQ channel model (14), (15) can be re-written as

$$P_{out}(\rho, \mathcal{R}) = \Pr \left\{ \frac{1}{2K} \mathcal{I} \left(\underline{z}; \underline{\mathbf{y}}_D^{equ,K} \mid \left\{ \mathbf{H}_l^{equ,K} \right\}, \rho \right) < \mathcal{R}, \bar{\mathcal{A}}_1, \dots, \bar{\mathcal{A}}_{K-1} \right\},$$

where $\bar{\mathcal{A}}_k$ represents the event that a NACK feedback is sent back to the source node S at round $k = 1, \dots, K - 1$.

Average Throughput

The average throughput formula corresponding to the transmission over the equivalent Relay ARQ MIMO channel is given by

$$\eta = \frac{\mathbb{E}[\mathcal{R}]}{\mathbb{E}[\nu]}. \quad (16)$$

- \mathcal{R} is a discrete random variable equals either to \mathcal{R} when successful packet decoding is detected within the K rounds or 0 otherwise.
- In an outage sense, these two values are taken with probabilities $1 - P_{out}(\rho, \mathcal{R})$ and $P_{out}(\rho, \mathcal{R})$, respectively.
- ν is a RV counting the number of rounds consumed to transmit one packet.

Thus, the **average throughput** (16) can be re-expressed as

$$\eta = \mathcal{R}_\nu (1 - P_{out}(\rho, \mathcal{R})) \quad (17)$$

where $\mathcal{R}_\nu = \mathcal{R}/\mathbb{E}[\nu]$.

Scenario 1

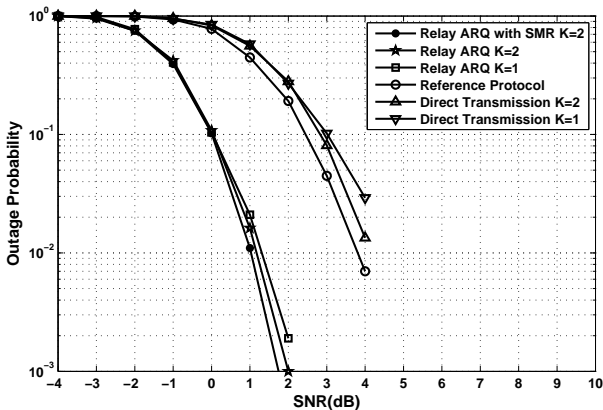


Fig. 4: Outage probability versus SNR for $l_{SR} = 0.3$, $N_S = N_R = N_D = 2$, $L_{SR} = L_{RD} = L_{SD} = 3$, and $\kappa = 3$.

Scenario 2

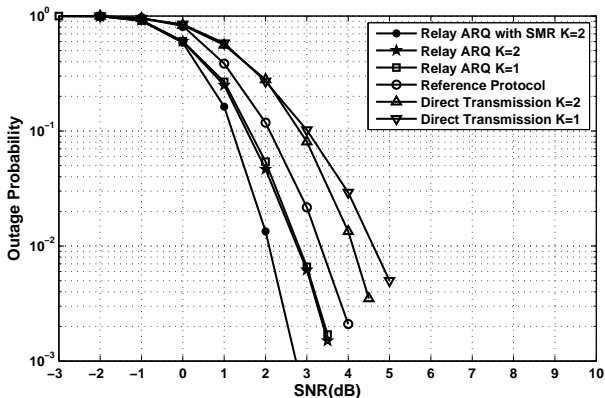


Fig. 5: Outage probability versus SNR for $l_{SR} = 0.7$, $N_S = N_R = N_D = 2$, $L_{SR} = L_{RD} = L_{SD} = 3$, and $\kappa = 3$.

Scenario 1

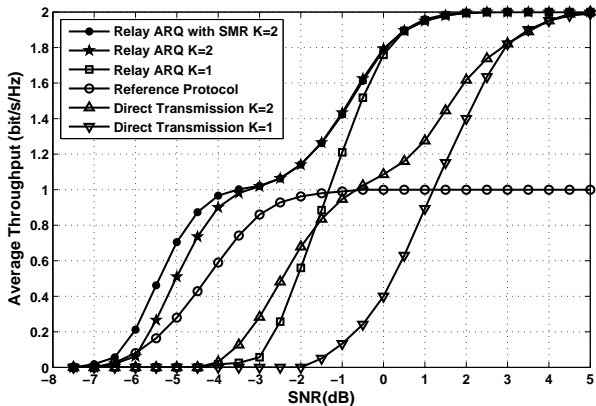


Fig. 6: Average throughput versus SNR for $l_{SR} = 0.3$, $N_S = N_R = N_D = 2$, $L_{SR} = L_{RD} = L_{SD} = 3$, and $\kappa = 3$.

Scenario 2

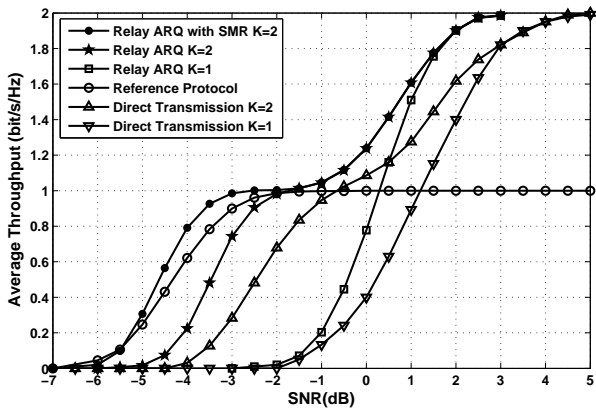


Fig. 7: Average throughput versus SNR for $l_{SR} = 0.7$, $N_S = N_R = N_D = 2$, $L_{SR} = L_{RD} = L_{SD} = 3$, and $\kappa = 3$.

Key Ideas

- One **time slot** \Rightarrow additional set of N_S transmit and N_D receive antennas at node S and Node D , respectively.
- One **packet re(transmission)** \Rightarrow additional set of $2N_D$ receive antennas at node D .

Our relay ARQ system at round $k \sim$ virtual $2N_D k \times 2N_S$ MIMO system

Soft Sub-Packet Combiner Derivation

- At ARQ round k , the $N_D k T \times N_S T$ sub-packet ARQ transmission model is given by

$$\underline{\mathbf{y}}^{equ,k} = \underline{\mathbf{H}}^{equ,k} \underline{\mathbf{z}} + \underline{\mathbf{n}}^{equ,k}, \quad (18)$$

where

$$\begin{cases} \underline{\mathbf{x}} = \underset{0 \leq t \leq \frac{T}{2}-1}{\text{clmn}}(\mathbf{z}_t) = \underset{0 \leq t \leq T-1}{\text{clmn}}(\mathbf{x}_t) \\ \underline{\mathbf{y}}^{equ,k} = \underset{0 \leq t \leq \frac{T}{2}-1}{\text{clmn}}(\mathbf{y}_{D,t}^{equ,k}) \\ \underline{\mathbf{n}}^{equ,k} = \underset{0 \leq t \leq \frac{T}{2}}{\text{clmn}}(\mathbf{n}_{D,t}^{equ,k}) \end{cases}. \quad (19)$$

- $\underline{\mathbf{H}}^{equ,k}$ can be block-diagonalized in the Fourier basis as

$$\underline{\mathbf{H}}^{equ,k} = \mathbf{U}_{T/2, 2N_D k}^H \underline{\Delta}^{(k)} \mathbf{U}_{T/2, 2N_S k}. \quad (20)$$

Soft Sub-Packet Combiner Derivation

- Applying the DFT to both sides of (18) yields the following multi-round frequency domain (FD) sub-packet ARQ transmission model

$$\underline{\mathbf{y}}_f^{equ,k} = \underline{\Delta}^{(k)} \underline{\mathbf{x}}_f + \underline{\mathbf{n}}_f^{equ,k}. \quad (21)$$

Unconditional MMSE Filter $\Rightarrow \tilde{\underline{\mathbf{x}}}_f^{(k)} = \Phi^{(k)} \underline{\mathbf{y}}_f^{equ,k} - \Psi^{(k)} \underline{\mathbf{x}}_f$

- The forward filter $\Phi^{(k)} = \text{diag} \left\{ \Phi_0^{(k)}, \dots, \Phi_{T/2-1}^{(k)} \right\}$, and the backward filter $\Psi^{(k)} = \text{diag} \left\{ \Psi_0^{(k)}, \dots, \Psi_{T/2-1}^{(k)} \right\}$ are respectively expressed, for $t = 0, \dots, T/2 - 1$, as

$$\begin{cases} \Phi_t^k = \frac{1}{N_0} \underline{\Delta}_t^{(k)H} \left\{ \mathbf{I}_{2N_D k} + \underline{\Delta}_t^{(k)} \mathbf{C}_t^{-1} \underline{\Delta}_t^{(k)H} \right\} \\ \mathbf{C}_t^{-1} = N_0 \tilde{\Theta}_{\underline{\mathbf{x}}}^{(k)-1} + \underline{\Delta}_t^{(k)H} \underline{\Delta}_t^{(k)} \\ \Psi_t^k = \Phi_t^{(k)} \underline{\Delta}_t^{(k)} - \frac{2}{T} \sum_{i=0}^{T/2-1} \Phi_i^{(k)} \underline{\Delta}_i^{(k)} \end{cases}.$$

Building Blocks of the Proposed Receiver

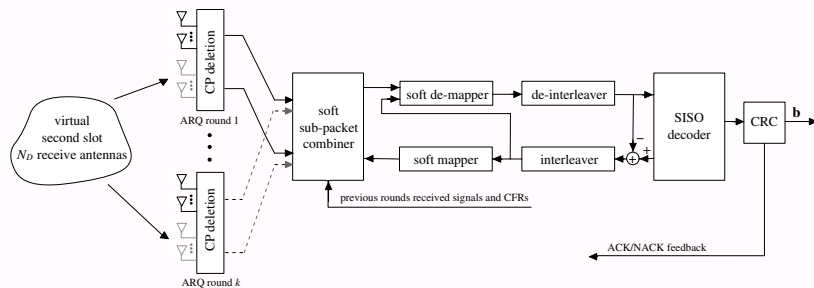


Fig. : Building blocks of the proposed turbo receiver.

Recursive Implementation (Algorithm)

- Two recursive variables: $\underline{\tilde{\mathbf{y}}}_t^{equ,k}$ and $\underline{\Gamma}^{(k)} = \text{diag} \left\{ \underline{\Gamma}_0^{(k)}, \dots, \underline{\Gamma}_{T/2-1}^{(k)} \right\}$ are introduced within the following new soft sub-packet combining structure

$$\underline{\tilde{\mathbf{x}}}_f^{(k)} = \underline{\tilde{\Phi}}^{(k)} \underline{\tilde{\mathbf{y}}}_f^{equ(k)} - \underline{\tilde{\Psi}}^{(k)} \underline{\tilde{\mathbf{x}}}_f, \quad (22)$$

where

$$\begin{cases} \underline{\tilde{\mathbf{y}}}_f^{equ(k)} = \underline{\tilde{\mathbf{y}}}_f^{equ(k-1)} + \underline{\Upsilon}^{(k)H} \underline{\mathbf{y}}_f^{equ(k)} \\ \underline{\tilde{\mathbf{y}}}_f^{equ(0)} = \mathbf{0}_{2N_S \times 1} \\ \underline{\Gamma}_t^{(k)} = \underline{\Gamma}_t^{(k-1)} + \underline{\Upsilon}_t^{(k)H} \underline{\Upsilon}_t^{(k)} \\ \underline{\Gamma}_t^{(0)} = \mathbf{0}_{2N_S \times 2N_S} \end{cases}$$

- The backward-forward filters have been adjusted to $\underline{\tilde{\Phi}}^{(k)} = \text{diag} \left\{ \underline{\tilde{\Phi}}_0^{(k)}, \dots, \underline{\tilde{\Phi}}_{T/2-1}^{(k)} \right\}$, and $\underline{\tilde{\Psi}}^{(k)} = \text{diag} \left\{ \underline{\tilde{\Psi}}_0^{(k)}, \dots, \underline{\tilde{\Psi}}_{T/2-1}^{(k)} \right\}$ with

$$\begin{cases} \underline{\tilde{\Phi}}_t^{(k)} = \frac{1}{N_0} \left\{ \mathbf{I}_{2N_S} - \underline{\Gamma}_t^{(k)} \mathbf{C}_t^{-1} \right\} \\ \mathbf{C}_i = N_0 \underline{\tilde{\Theta}}_{\underline{\tilde{\mathbf{x}}}}^{k-1} + \underline{\Gamma}_t^{(k)} \\ \underline{\tilde{\Psi}}_t^{(k)} = \underline{\tilde{\Phi}}_t^{(k)} \underline{\Gamma}_t^{(k)} - \frac{2}{T} \sum_{t=0}^{T/2-1} \underline{\tilde{\Phi}}_t^{(k)} \underline{\Gamma}_t^{(k)} \end{cases}$$

Scenario 1

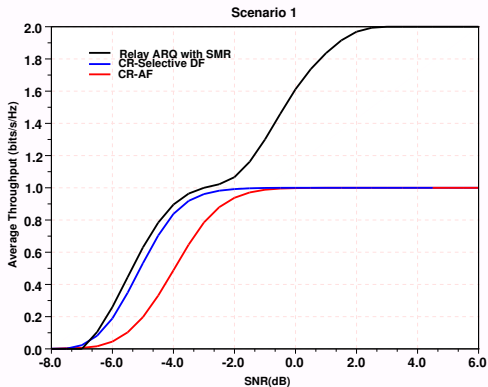


Fig. 6: Average throughput versus SNR for $l_{SR} = 0.3$, $N_S = N_R = 2$, $N_D = 3$, $L_{SR} = L_{RD} = L_{SD} = 3$, and $\kappa = 3$.

Scenario 2

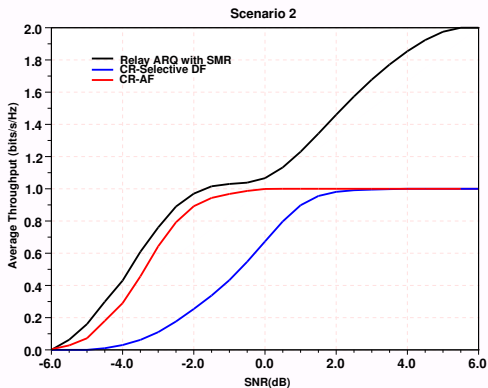


Fig. 7: Average throughput versus SNR for $l_{SR} = 0.6$, $N_S = N_R = 2$, $N_D = 3$, $L_{SR} = L_{RD} = L_{SD} = 3$, and $\kappa = 3$.

Conclusion

- **New throughput-efficient relay ARQ techniques are investigated.**
- The half-duplex constraint has been turned from a disadvantage causing a multiplexing gain loss to an advantage providing significant improvement in average throughput & outage probability performance.
- Relay ARQ with SMR along with signal-level turbo sub-packet combining provides considerable gain in average throughput compared with conventional ARQ-based cooperative relaying over the entire SNR region.

Conclusion

- **New throughput-efficient relay ARQ techniques are investigated.**
- **The half-duplex constraint has been turned from a disadvantage causing a multiplexing gain loss to an advantage providing significant improvement in average throughput & outage probability performance.**
- Relay ARQ with SMR along with signal-level turbo sub-packet combining provides considerable gain in average throughput compared with conventional ARQ-based cooperative relaying over the entire SNR region.

Conclusion

- **New throughput-efficient relay ARQ techniques are investigated.**
- **The half-duplex constraint has been turned from a disadvantage causing a multiplexing gain loss to an advantage providing significant improvement in average throughput & outage probability performance.**
- **Relay ARQ with SMR along with signal-level turbo sub-packet combining provides considerable gain in average throughput compared with conventional ARQ-based cooperative relaying over the entire SNR region.**

Perspectives

- Analytical results of the outage probability and average throughput instead of Monte-Carlo based simulations should be investigated.
- Extension of the proposed techniques to a multi-user environment where several relays are deployed.

Perspectives

- **Analytical results of the outage probability and average throughput instead of Monte-Carlo based simulations should be investigated.**
- Extension of the proposed techniques to a multi-user environment where several relays are deployed.

Perspectives

- **Analytical results of the outage probability and average throughput instead of Monte-Carlo based simulations should be investigated.**
- **Extension of the proposed techniques to a multi-user environment where several relays are deployed.**

Related Works

- **Zakaria El-Moutaouakkil**, Tarik Ait-Idir, Halim Yanikomeroglu, and Samir Saoudi, "*Receiver Design for Throughput-Efficient MIMO Relay ARQ Transmissions*," to be submitted, IEEE Transactions on Signal Processing, 30 pp., December 2012.
- Hatim Chergui, Tarik Ait-Idir, Mustapha Benjillali, **Zakaria El-Moutaouakkil**, and Samir Saoudi, "*Joint-Over-Transmissions Project and Forward Relaying for Single Carrier Broadband MIMO ARQ Systems*," submitted, IEEE Vehicular Technology Conference VTC-Spring 2011, Budapest, Hungary, May 2011.
- **Zakaria El-Moutaouakkil**, Tarik Ait-Idir, Halim Yanikomeroglu, and Samir Saoudi, "*Relay ARQ Strategies for Single Carrier MIMO Broadband Amplify-and-Forward Cooperative Transmission*," in Proc., 21th Annual IEEE Symposium on Personal Indoor and Mobile Radio Communications PIMRC 2010, Istanbul, Turkey, Sep. 2010.
- Tarik Ait-Idir, Houda Chafnaji, and Samir Saoudi, "*Turbo Packet Combining for Broadband Space-Time BICM Hybrid-ARQ Systems with Co-Channel Interference*," IEEE Transactions on Wireless Communications, vol. 9, no. 5, pp. 1686-1697, May 2010.

Perspectives & Conclusion

Thank you very much